pK_a Perturbation in Genomic Hepatitis Delta Virus Ribozyme Catalysis Evidenced by Nucleotide Analogue Interference Mapping†

Adegboyega K. Oyelere,‡ Julia R. Kardon, and Scott A. Strobel*

Department of Molecular Biophysics and Biochemistry and Department of Chemistry, Yale University, 260 Whitney Avenue, New Haven, Connecticut 06520-8114

Received September 19, 2001; Revised Manuscript Received December 26, 2001

ABSTRACT: The Hepatitis Delta Virus (HDV) ribozyme was the first RNA enzyme proposed to use a proton-transfer mechanism for catalysis. Previous biochemical evidence suggested that the genomic HDV ribozyme promotes cis-cleavage using cytosine 75 whose pK_a is perturbed within the active site. Here we present further biochemical evidence for the involvement of C75 in proton transfer, as well as evidence to support a plausible mechanism for C75 pK_a perturbation. Nucleotide analogue interference mapping (NAIM) experiments with C analogues having altered N3 pK_as demonstrate the importance of C75 ionization in the HDV cis-cleavage reaction. pH-dependent interference rescue with C analogues having enhanced N3 acidity indicates that C75 is the only cytidine residue that must be protonated for ribozyme activity. Furthermore, interference analysis with pseudoisocytidine, a charge-neutral mimic of a C with a protonated N3, shows a pattern consistent with proton transfer, possibly from the C75 N3 to the 5′-oxyanion leaving group during the cis-cleavage reaction. Strong pH-independent inhibition of ribozyme function also occurs at C75 with a C analogue that lacks the N4 amino group, implicating the exocyclic amine in critical interactions in the active site. Interactions with the amino group may play an important role in perturbing the C75 N3 pK_a. Protonation of C41 has been proposed to be important for ribozyme activity; however, no interference at C41 was observed in this analogue series, which argues against a functional role for C41 protonation. These data support a model wherein C75 of the genomic HDV ribozyme acts as a general acid during its cis-cleavage reaction, and provide a glimpse into how RNAs, in a manner similar to protein enzymes, might employ local environmental electronic modulation to catalyze reactions.

Protein enzymes efficiently facilitate proton transfer and use it to catalyze a wide range of biochemical reactions. The three-dimensional structure can accommodate exogenous cofactors (*1*) or accurately position ionizable side chains with near-neutral acidity constants for use in chemical reactions (*2*). Furthermore, the microenvironment of the active sites can lead to pK_a perturbation of side chain functional groups, activating them for catalysis (*3*). Charge redistribution through proton transfer is necessary to drive phosphodiester transfer reactions, and protein enzymes often catalyze these reactions through general acid−base mechanisms (*4*, *5*).

Catalytic function is not unique to protein enzymes. Several RNA-based catalysts (ribozymes) exist in nature that catalyze phosphodiester transfer reactions (*6*−*8*); however, RNAs lack functional groups with near-neutral pK_as (*9*). This places them at an apparent disadvantage in their ability to use proton-transfer mechanisms at physiological pH, though biochemical and structural studies have revealed that folded RNAs can create microenvironments leading to pK_a perturbation of heterocyclic ring functional groups (for examples of pK_a perturbation in RNAs, see *10*−*15*). These observations open the possibility that RNA functional groups may participate in proton-transfer mechanisms to facilitate catalysis.

The common sites of pK_a perturbation in RNA are the N1 of adenine and the N3 of cytosine. Near-neutral pK_as have been observed at these two positions in different RNAs (*10*−*15*). Many of these pK_a-perturbed sites are likely to play only structural roles because they are involved in hydrogen-bonding interactions. Recent developments in catalytic RNA biochemistry and structural biology increasingly suggest that proton transfer is a viable catalytic mechanism utilized by ribozymes to promote chemical reactions (*16*−*21*). For example, it has been shown that some small ribozymes are active in the absence of divalent metals ions, which has led to the suggestion that they may be using RNA functional groups to mediate catalysis (*17*, *22*−*24*).

One ribozyme that has been proposed to directly utilize RNA functional groups for catalysis is the self-cleaving RNA from the Hepatitis Delta Virus (HDV).[1] HDV is a pathogen closely associated with the virulence of hepatitis B infection in humans (*25*). It is an RNA virus whose genome contains a single-stranded RNA molecule (ca. 1700 nt) that is

† Supported by NSF Grant CHE 0100057 to S.A.S. and by a postdoctoral fellowship from the Jane Coffin Childs Memorial Fund for Medical Research to A.K.O.

* To whom correspondence should be addressed. Phone: (203)432-9772. FAX: (203)432-5767. Email: strobel@csb.yale.edu.

‡ Present address: Rib-X Pharmaceuticals, Inc., 25 Science Park, New Haven, CT 06511.

[1] Abbreviations: HDV, Hepatitis Delta Virus; NAIM, nucleotide analogue interference mapping; n^6C, 6-azacytidine; f^5C, 5-fluorocytidine; Z, zebularine; ΨiC, pseudoisocytidine; C, cytidine; n^6CαS, 6-azacytidine-5′-*O*-phosphorothioate; f^5CαS, 5-fluorocytidine-5′-*O*-phosphorothioate; ZαS, zebularine-5′-*O*-phosphorothioate; CαS, cytidine-5′-*O*-phosphorothioate; PAGE, polyacrylamide gel electrophoresis.

10.1021/bi011816v CCC: $22.00
Published on Web 02/08/2002

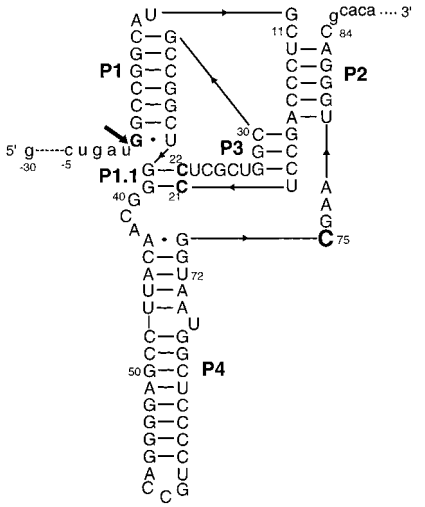

FIGURE 1: Secondary structure of the genomic HDV ribozyme (*16*). The site of the ribozyme cis-cleavage reaction is indicated with a heavy arrow. Nucleotide numbering starts at the cleavage site with the ribozyme sequence represented in upper case letters, while sequences flanking the ribozyme are denoted in lower case letters. Paired regions are labeled P, and thin lines with arrows trace the connections between sequence elements.

replicated by a rolling cycle mechanism (*26*). Both the genomic and the antigenomic RNA strands of HDV are capable of catalyzing a self-cleavage reaction. Their catalytic activities reside within a continuous 85 nucleotide long ribozyme sequence (Figure 1) (*27*, *28*), which performs a cis-cleavage reaction leading to the formation of 2′,3′-cyclic phosphate and 5′-hydroxyl cleaved products. The structure of the cleaved genomic HDV ribozyme was determined at 2.3 Å resolution (*16*), which revealed that the heterocyclic base of a cytidine residue, C75, is situated within an active site cleft (*16*). Moreover, the N3 of C75 is within hydrogen-bonding distance of the leaving 5′-hydroxyl group. Based on these observations, it was hypothesized that the cis-cleavage reaction of the HDV ribozyme utilizes the N3 of C75 possibly via a general acid or general base mechanism (*16*).

This hypothesis was corroborated by biochemical and mutagenesis studies (*17*, *18*). The macroscopic pK_a of the HDV ribozyme cis-cleavage reaction has been estimated to approach neutrality in reactions containing low concentrations of divalent metal ions (*17*). The replacement of C75 with U completely eliminated ribozyme function, consistent with the inability of uridine (N3 pK_a = 9.4) to be involved in proton transfer under neutral to slightly basic conditions (*17*, *18*). Conversely, some rescue of function has been observed in the presence of exogenous bases with near-neutral pK_as (*18*, *29*).

We sought to further explore the functional relevance of base ionization at C75 and other residues in the genomic HDV ribozyme using nucleotide analogue interference mapping (NAIM) analysis (*30*). The particular advantage of NAIM for such an application is that it is possible to explore the effect of analogue substitution simultaneously, yet individually, at every position within an RNA molecule. We have reported a series of nucleotide analogues that retain the hydrogen-bonding potential of cytidine, but that have altered pK_as. Because the extent and mechanisms of pK_a perturbation in RNAs vary with local sequence and structure, it is desirable to have a set of nucleoside analogues that are sensitive to both subtle and gross pK_a variations. The analogues must also have a broad range of N3 pK_a values but with substantially different causes for the pK_a shift (Figure 2). For example, substitution of the C6 with nitrogen or replacement of the C5 hydrogen with fluorine causes enhanced acidity at N3 in the analogues 6-azacytidine (n^{6}CαS, N3 pK_a = 2.6) and 5-fluorocytidine (f^{5}CαS, N3 pK_a = 2.3), respectively (*31*, *32*). This compares to an N3 pK_a of 4.2 for cytidine (*33*). Despite this change in pK_a, the Watson−Crick hydrogen-bonding faces of both analogues are unaffected. Alternatively, deletion of the N4 group enhances the acidity at N3 in the analogue zebularine (ZαS, N3 pK_a = 2.5) (*34*), but it also reduces its Watson−Crick hydrogen-bonding ability (*35*). Conversely, pseudoisocytidine (ΨiCαS, N3 pK_a = 9.4) is a C-linked nucleoside that predominantly exists as a charge-neutral mimic of N3-protonated C due to enhanced basicity at N3 (*30*, *36*−*38*).

The interference pattern produced by this collection of analogues was previously calibrated on a mutant form of the *Tetrahymena* group I intron that contains a C300+G97−C277 triple within its active site (*30*, *39*). In this system, the microenvironment of C300 raises the N3 pK_a, which facilitates Hoogsteen hydrogen bonding with G97. These data were used to define the interference pattern characteristic of a C with an elevated N3 pK_a essential to ribozyme function. First, f^{5}CαS and n^{6}CαS cause interference under slightly alkaline pH conditions due to the reduced protonation efficiency of both analogues. Because f^{5}CαS and n^{6}CαS both retain a complete set of Watson−Crick hydrogen-bonding groups, neither of these analogues were observed to cause interference within base-pairing regions (*30*). Second, in cases where interference is due to a pK_a effect, the interference is reduced or eliminated when the NAIM experiment is performed at acidic pHs. The pH dependence of the interference makes it possible to distinguish between effects due to base protonation versus inhibition resulting from either the 5-fluoro or the 6-imino group substitution. Third, ZαS incorporation into sites where N3 pK_a perturbation is essential to RNA function leads to interference, but the interference is pH-insensitive if the N4 group is involved in the mechanism of pK_a perturbation or in important hydrogen-bonding interactions. In general, ZαS does not cause

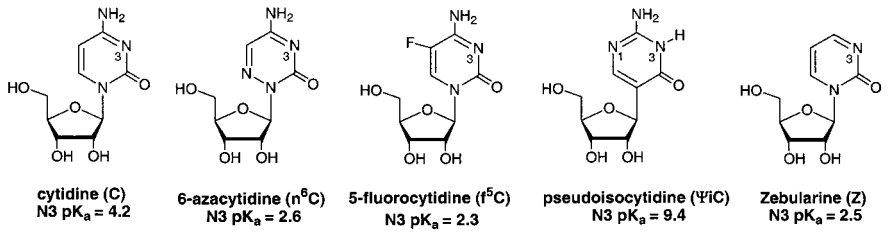

FIGURE 2: Nucleoside analogues and their abbreviations: cytidine, 6-azacytidine, 5-fluorocytidine, pseudoisocytidine, and zebularine. The unperturbed pK_a of the N3 imino group is specified for all nucleosides.

interference within duplex regions, though a few exceptions within the *Tetrahymena* group I intron have been observed (A.K.O. and S.A.S., unpublished results). Fourth, ΨiCαS results in enhanced activity (scored as increased band intensity in the phosphorothioate cleavage ladder) at alkaline pHs due to the presence of the N3 proton in this uncharged mimic of a protonated C. Enhancement is diminished as the pH is reduced. Although the N3 tautomer of ΨiCαS is preferred, the N1 tautomer can form, which makes it possible for the analogue to be efficiently incorporated into RNA opposite G. Consistent with this observation, no ΨiCαS interference was observed within duplex regions (*30*).

Nakano et al. (*17*) postulated that general acid catalysis of the genomic HDV cleavage reaction is limiting in the absence of divalent metal ions, while the effect of the unprotonated general base becomes limiting in the presence of divalent metal ions. Recent observations by Wadkins et al. (*40*), however, suggested that a pH-sensitive interaction involving a protonated C41 may be limiting in the cis-cleavage reaction performed in the absence of divalent metal ions. It is therefore interesting to compare the interference patterns under both divalent and monovalent ion conditions and to investigate the possibility of base ionization at every position in the ribozyme, not just C75. This collection of analogues, each tagged with a phosphorothioate group for use in NAIM, provides a straightforward means to achieve this objective. Here we report that the interference pattern supports the model, wherein the C75 of the HDV ribozyme acts as a general acid during the cis-cleavage reaction (*17*).

MATERIALS AND METHODS

Chemicals and Biochemicals. Nucleoside triphosphates and molecular biology grade reagents were purchased from Sigma. Doubly deionized water was obtained from a Millipore Ultra water purification system. Restriction enzymes and T4-RNA ligase were procured from New England Biolabs and used according to manufacturer protocols. DNA oligonucleotides were purchased from the Keck oligonucleotide facility (Yale University, New Haven). Pseudoisocytidine was purchased from Berry & Associates (Ann Arbor, MI). All other chemical reagents were from Aldrich and used without further purification.

Nucleotide Analogue Synthesis. Details of the synthesis of the 5′-*O*-(1-thio)triphosphate derivatives of C, f^{5}C, n^{6}C, and ΨiC have been previously reported (*30*). The 5′-*O*-(1-thio)triphosphate derivative of Z was synthesized using a modification of the Arabshahi and Frey procedure (*30*, *41*).

Preparation of Ribozymes. Plasmid containing wild-type genomic −30 to +99 HDV sequence upstream of a T7 promoter was linearized with *Bfa*I to generate the +99 end (*17*). Ribozymes were prepared by T7 RNA polymerase transcription of the digested plasmid. For NAIM experiments, 5′-*O*-phosphorothioate (αS) derivatives of C, f^{5}C, n^{6}C, ΨiC, and Z were randomly incorporated into RNA transcripts by runoff transcription as previously described (*30*, *39*). RNA transcripts were 3′ end labeled with [α-^{32}P]dATP using T7 DNA Sequenase (USB) in the presence of an oligonucleotide splint, T3HDV-PB (ATTAGAGAGATTTGTGGG), which is complementary to the 17-nucleotide sequence at the 3′ end of the HDV ribozyme (*42*, *43*). The small amount of residual cis-cleavage during transcription of the HDV transcripts was eliminated by including a DNA oligonucleotide (T3HDV-PB) complementary to the 17-nucleotide sequence at the 3′ end of the ribozyme. T3HDV-PB was eliminated by gel purification prior to NAIM analysis.

NAIM Analysis of the HDV Ribozyme cis-Cleavage Reaction. Interference experiments were performed in reaction buffers ranging between pH 4.0 and 8.5. Tris-HCl (40 mM) was used at pH 7.5 and 8.5, MES (25 mM) at pH 5.0 and 6.5, HEPES (50 mM) at pH 7.0, and NaOAc (40 mM) at pH 4.0. The HDV cleavage reaction was induced at 37 °C by adding a saturating concentration of DNA oligonucleotide, AS-1 (TAAGAAAGGATGGAACGCGGACCCCCA CAC), as described by Nakano et al. (*17*). Cleavage reactions were performed with divalent metal ions (1−10 mM $MgCl_2$) or monovalent metal ions (1 M NaCl, 1 mM EDTA) (*17*). To ensure the same extent of reaction at all pHs for the NAIM assay, incubation times were identified that gave about 60% cleaved product. For experiments performed in 1 mM $MgCl_2$, incubation times of 10 and 180 min were sufficient at pH 8.5 and 5.0, respectively. In 1 M NaCl, 1 h incubation was sufficient at pH 5.0, while a 16 h incubation was necessary for experiments at pH 4.0 and 7.5. The reactions were quenched by adding 30 mM EDTA and formamide loading buffer (*17*), and the reaction products were separated on denaturing 8% PAGE. Both the cut and uncut RNAs were excised from the gel, eluted into 2% SDS, and isolated as described (*30*). The phosphorothioate linkages in the cut and uncut RNAs were cleaved with I_2, and the products were resolved by denaturing 8% PAGE.

Gel peak intensities for each of the I_2-cleaved products were quantitated on a Storm PhosphorImager (Molecular Dynamics). The relative partition (Π) between the uncut and cut RNAs for each analogue at each position was used to calculate the extent of interference as a ratio:

$$\Pi = (\text{analogue peak intensity uncut RNA}/\text{analogue peak intensity cut RNA})/(\text{phosphorothioate peak intensity uncut RNA}/\text{phosphorothioate peak intensity cut RNA})$$

A Π value of 1 corresponds to an equal partition and no analogue interference, while a value of approximately 2 is considered interference. A Π value less than 0.5 corresponds to enhancement of ribozyme function. For effects resulting from phosphorothioate effects, Π was calculated simply as the ratio of peak intensity for the uncut versus the cut RNAs.

RESULTS

Kinetic Reaction Profile of the HDV Ribozyme Construct. For this study, we utilized the HDV ribozyme construct kinetically characterized by Nakano et al. (*17*). This ribozyme includes nucleotides −30 to +99 and is inactive until a DNA oligonucleotide (AS-1) complementary to the 5′ end of the ribozyme is added (*17*). In the presence of Mg^{2+} ion, the logarithm of the observed rate constant for this ribozyme increases with a slope of ≈1 between pH 4.5 and 6. The rate is pH-insensitive from pH 7 to 8.5, and the reaction pK_a is ≈6.8 at 1 mM Mg^{2+} (*17*). Nakano reported a substantial deuterium isotope effect throughout the pH range, which indicates that the pK_a is due to an ionization event rather than a change in the rate-limiting step (*17*). In the absence

of divalent metal ion (1 M NaCl), the observed rate decreases with pH at a slope of ≈−1 between pH 6 and 8. This condition was proposed to unmask the underlying general acid catalysis, though alternative explanations involving structural protonation of C41 have also been suggested (*40*).

Interference Analyses with pK_a-Perturbed C Analogues. We investigated the role played by base ionization in the HDV ribozyme cis-cleavage reaction by determining the effects of incorporating C analogues with N3 pK_a perturbations, individually yet simultaneously, at every position in the genomic HDV ribozyme. Ribozymes with a 3′ end label and a random distribution of either CαS or any of the four phosphorothioate-tagged pK_a-perturbed C analogues were induced for cis-cleavage by adding DNA oligonucleotide AS-1 (*17*). This produced about 60% cleaved product under monovalent (1 M NaCl, 1 mM EDTA) and divalent metal ion (1−10 mM $MgCl_2$) conditions. Cut and uncut RNAs were separated and subjected to NAIM analysis at every C in the genomic HDV ribozyme between positions +1 and +84 (*30*, *44*−*46*). This included 22 C's involved in Watson−Crick base pairs and 8 C's located in single-stranded regions or involved in noncanonical base pairs (*16*). In summary, a pH-dependent interference was seen only at a single base, C75, a cytidine residue predicted to be catalytically important. C21 and C22 displayed pH-independent analogue-specific inhibition of ribozyme function. No interference was observed at C41 or any other nucleotide in the RNA. A description follows of the specific interference patterns observed throughout the RNA.

Interference Analysis in P1.1. C21 and C22 are involved in Watson−Crick base pairs with G39 and G38, which form the nested pseudoknot helix P1.1 (*16*) (Figure 1). NAIM analysis of reactions performed in 1 M NaCl revealed a strong pH-independent phosphorothioate effect at C22 consistent with a previous report (see Supporting Information) (*47*). The effect was substantially lower for RNAs reacted in 1 mM Mg^{2+}, consistent with a possible RNA folding effect (Figures 3a and 4). Interference beyond that due to the phosphorothioate effect resulted from ΨiCαS and ZαS substitution at C22, though no effects were seen with f^5CαS or n^6CαS. Instead, n^6CαS interfered with ribozyme function at the neighboring nucleotide in the P1.1 helix, C21, but none of the other analogues, including f^5CαS, showed an effect at this position (Figure 3a). All of the interferences in the P1.1 region persisted independent of the reaction pH (Figure 3b, Figure 4, right panels). The lack of f^5CαS interference suggests that the pH-independent interferences of ΨiCαS and n^6CαS at C22 and C21, respectively, are due to the extra modifications on the non-Watson−Crick face of their pyrimidine rings. ZαS interference at C22 is likely due to the weakening of the C22-G38 base pair at the P1.1 helix region of the ribozyme, a direct consequence of removing the N4 group (*35*). ZαS interference is not observed at every G-C pair, but the P1.1 helix is particularly short (2 base pairs) and hence may be unusually susceptible to secondary structure effects. Thus, while some interferences occur in the P1.1 helix, the pattern is inconsistent with an important ionization event.

Lack of Interference at C41. The crystal structure of the cleaved genomic HDV ribozyme revealed that C41 is involved in base quadruple interactions that may be stabilized by protonation of its N3 (*16*). Protonation of C41 has been

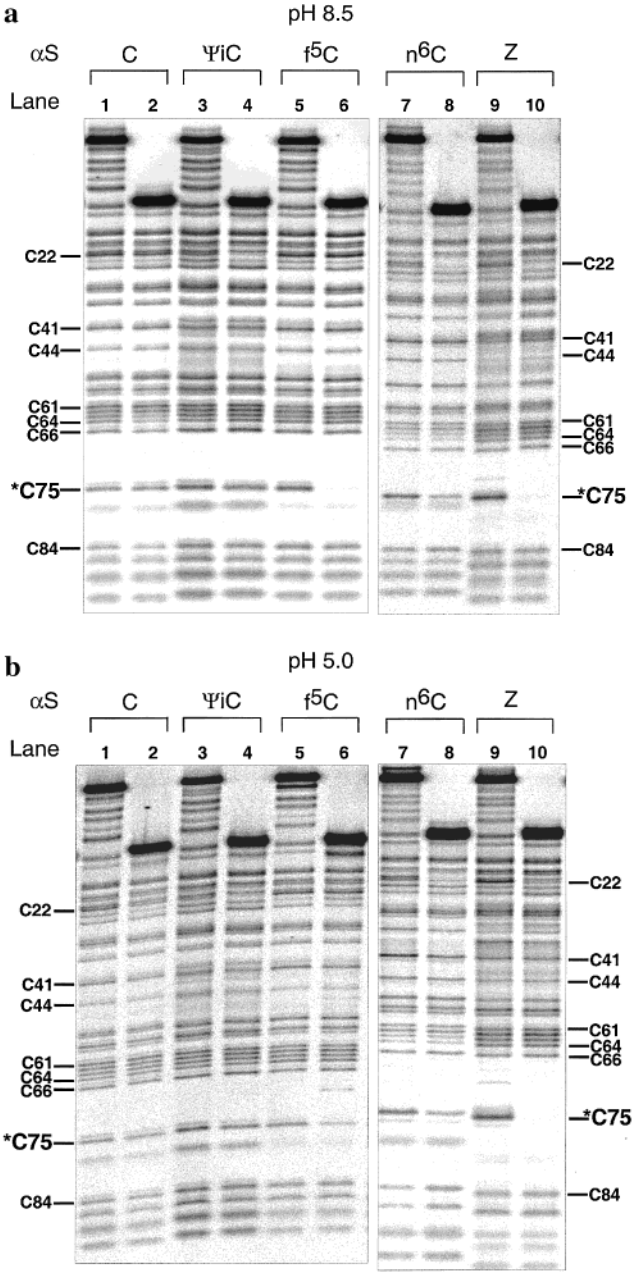

FIGURE 3: NAIM analysis of the HDV ribozyme. Autoradiographs of I_2-treated RNA containing CαS, ΨiCαS, f^5CαS, n^6CαS, or ZαS. RNAs that remained uncut during the HDV ribozyme cis-cleavage reaction are shown in the odd-numbered lanes, while RNAs that were cut are in even-numbered lanes. (a) Reaction at pH 8.5. (b) Reaction at pH 5.0. Bands corresponding to specific nucleotide positions are identified to the left with the single site of pH-dependent interference rescue, C75, marked with an asterisk. The analogue that is incorporated into the RNA and the pH of the reaction are specified above the gel. These experiments were performed in 1 mM Mg^{2+} with incubation times of 10 and 180 min at pH 8.5 and 5.0, respectively.

suggested to be important and limiting under monovalent ion conditions (*40*). This possibility was directly explored using this analogue series. We observed no analogue interferences at C41 at neutral to alkaline pHs in 1 M NaCl. Instead, moderate but inconsistent interference resulted from incorporation of f^5CαS, n^6CαS, and ZαS at acidic pHs (4.0−5.0) (data not shown, see Supporting Information). No interference was observed at C41 in reactions containing 1 mM Mg^{2+} (Figures 3 and 4). These observations suggest

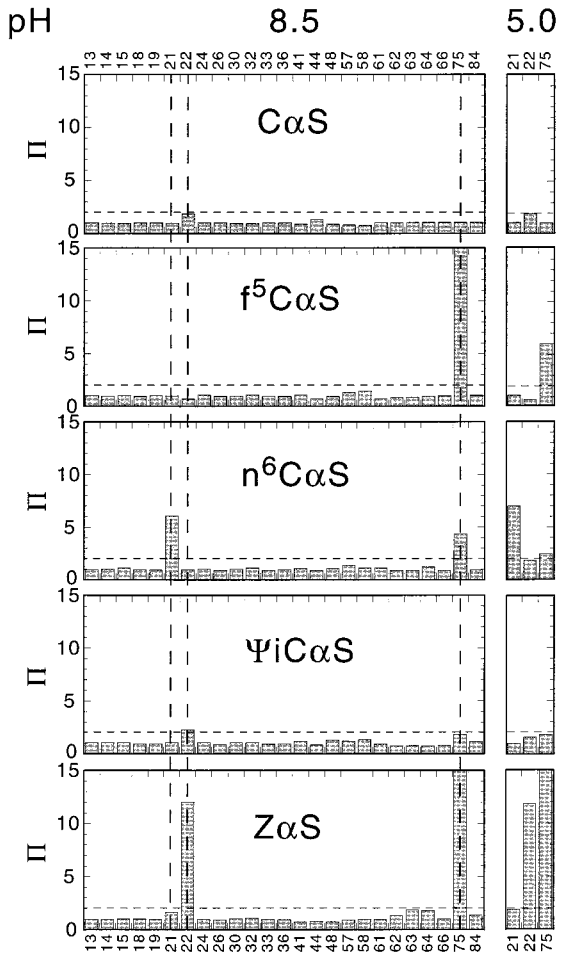

FIGURE 4: Histograms indicating the partition values, Π, at all C's throughout the HDV ribozyme at pH 8.5 (left) and at selected C's (21, 22, and 75) at pH 5.0 (right). The identity of the analogue in each experiment is indicated. Complete interference in this system corresponds to a value of 15.

that C41 protonation is neither structurally nor catalytically important for the HDV ribozyme cis-cleavage reaction. In fact, interference at low pH suggests that C41 protonation may be somewhat inhibitory, possibly due to stabilization of an inactive RNA conformation upon C41 protonation.

Interference Analysis of the Active Site C75. C75 is a critical residue buried in the active site cleft where it is positioned to act catalytically (*16*). We observed that ribozyme function was inhibited when either n^6CαS or f^5CαS was incorporated at C75 (Figure 3a, lanes 6 and 8). This occurred in both divalent (1 mM $MgCl_2$, pH 8.5) (Figure 3a) and monovalent (1 M NaCl, pH 7.5) (Supporting Information) metal ion conditions at high pH. The extent of interference in 1 mM Mg^{2+} ion at pH 8.5 was greater for f^5CαS (Π = 15) compared to n^6CαS (Π = 4.5) (Figure 4). If interference is caused by an N3 pK_a effect, then reducing the reaction pH should increase the population of protonated analogue and eliminate or significantly reduce the level of interference (*30*). To explore the pH dependence of C75 interference, the analysis was repeated with n^6CαS and f^5CαS at acidic pHs. In experiments performed in 1 mM Mg^{2+} ion, C75 interference persisted at pH 7 and 6, but the interference was notably suppressed at pH 5.0 (Figure 3b, lanes 6 and 8, Figure 4, right panels). In 1 M NaCl, C75 interference persisted down to pH 4.5, but was mostly suppressed at pH 4.0 (Supporting Information). Again a difference was observed in the extent of interference, with f^5CαS having a higher Π value (Π = 6.0) compared to n^6CαS (Π = 2.5) (Figure 4). This difference in the efficiency of interference rescue was also observed within the *Tetrahymena* ribozyme (*30*). This indicates that the C75 N3 pK_a is important to the HDV cis-cleavage reaction under both monovalent and divalent reaction conditions, although the efficiency and pH of the rescue were somewhat condition-dependent. These results are consistent with C75 protonation being required for proper functioning in the wild-type HDV ribozyme under both reaction conditions.

NAIM analysis was also performed with ZαS to explore the possible importance of the C75 exocyclic amine. ZαS lacks the N4 amine, but its N3 pK_a (pK_a = 2.5) is similar to that of n^6CαS (pK_a = 2.6), whose N4 group is unaltered (Figure 2). ZαS resulted in complete inhibition of ribozyme function at C75, but the inhibitory effect was not alleviated at any pH tested (Figure 3a,b, compare lanes 9 and 10, Figure 4). Given that an analogue with a similar pK_a can be rescued by altering the reaction pH, this result points to the importance of the C75 N4 group within the HDV ribozyme active site.

Given the similarity between these HDV C75 and the *Tetrahymena* C300 interference data, ΨiCαS incorporation at C75 might be expected to lead to pH-dependent enhancement as was observed in the group I intron model system. In that case, protonation of C300 plays a structural role in the formation of the C300+G97 Hoogsteen base pair. ΨiCαS incorporation at C300 provided a competitive advantage because the major tautomeric form of ΨiC, unlike C, is protonated without the need to perturb the nucleotide's pK_a. In contrast to this simple prediction, incorporation of ΨiCαS at C75 resulted in moderate interference. This was true in reactions containing either divalent or monovalent metal ions. Furthermore, the magnitude of the interference persisted at the same level at all pHs investigated (Figure 3a,b, compare lanes 3 and 4, Figure 4). Thus, ΨiCαS interference at HDV C75 was altogether different than that of *Tetrahymena* C300. This suggests that while C protonation contributes to ribozyme function in both systems, the role played by protonation is not equivalent.

DISCUSSION

An understanding of the mechanism of base pK_a perturbation in small catalytic RNAs may have direct implications for understanding the catalytic mechanisms of large RNAs, including the ribosome (*19*). It may also be helpful for formulating general rules regarding proton transfer in RNA catalysis. Toward this goal, we set out to investigate the role of base ionization and proton transfer during the genomic HDV ribozyme cis-cleavage reaction. Because RNAs lack functional groups with near-neutral pK_as comparable to those present in protein enzymes, it has been thought that they were unable to efficiently utilize charge-transfer mechanisms to catalyze chemical reactions. Their catalytic potential was considered to reside solely in their ability to position substrates near catalytic metal ion cofactors (*5*). However, recent crystallographic and biochemical studies on the HDV ribozyme gave evidence for the involvement of the C75 N3 in a proton-transfer process during its cis-cleavage reaction

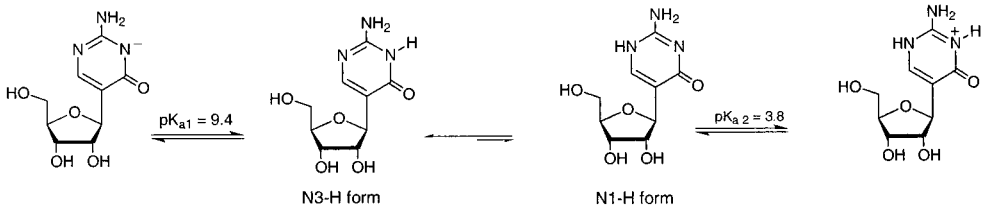

FIGURE 5: Tautomeric and equilibrium forms of pseudoisocytidine. Pseudoisocytidine exists in two tautomeric forms termed N3−H and N1−H. The pK_a of the Watson−Crick face of both forms is indicated as is the equilibrium between the two tautomeric forms, which depends on the polarity of the solvent (*38*). The N3−H tautomer form is favored (*38*).

(*16*−*18*, *29*). This conclusion is further supported by the data presented here.

C75 Protonation Is Important to HDV Ribozyme Function. The interference data fully support the conclusion that protonation of C75 is important for genomic HDV ribozyme function. We find that incorporation of C analogues with enhanced N3 acidity at C75 significantly interferes with ribozyme function at slightly basic and neutral pHs, while interference can be partially rescued at acidic pHs. A direct correlation between the catalytic integrity and protonation state of C75 N3 in HDV ribozyme is apparent in the difference in the interference magnitude between n^6CαS and f^5CαS at alkaline pH. This may be due to a higher population of catalytically active N3 protonated species in n^6CαS compared to f^5CαS after active site pK_a perturbation. A similar differential interference between n^6CαS and f^5CαS has been observed at a site within the *Tetrahymena* group I intron where base ionization is essential to function (*30*). The observation that the C75-substituted ribozymes are most active at low pH argues that C75 must be or become protonated at some stage along the reaction profile. In contrast to C75, no interference at C41 was observed with n^6CαS and f^5CαS at high pH where these analogues are unlikely to be protonated, which argues against a functional role for C41 protonation in the genomic ribozyme.

Deletion of the C75 N4 group has a dramatic pH-independent effect on ribozyme activity. As seen in the crystal structure of the cleaved form of the HDV ribozyme, a hydrogen-bonding interaction between the trans face of the C75 N4 group and the *pro-*R_P oxygen of C22 is part of a network of interactions critical for the organization of the ribozyme active site (*16*). This interference suggests that the proper positioning of C75 at the HDV ribozyme active site is essential to ribozyme function. In addition, the hydrogen-bonding interaction between the anionic *pro-*R_P oxygen of C22 and the hydrogen atom attached to an electron-donating N4 of C75 may modulate the electron-donating ability of N4 and by consequence affect the pK_a of N3 (*5*, *17*). Such charge-side-chain placement mechanisms have been successfully exploited to effect amino acid side chain pK_a perturbation in protein enzymes, such as acetoacetate decarboxylases (*3*). At the very least, correct folding of the active site, involving direct participation of the base functional groups of C75, appears to be essential for the creation of a microenvironment suitable for effective catalysis.

Evidence in Support of C75 Proton Transfer. While these interference data argue that the pK_a of C75 is perturbed and that the perturbation is functionally important, they do not distinguish whether C75 protonation plays a structural or a more direct catalytic role for ribozyme activity. In an effort to distinguish these two possibilities for the HDV ribozyme, we performed NAIM analysis with ΨiCαS. Based upon previous work on model systems, C's that are ionized for strictly structural purposes, i.e., the proton is used for hydrogen bonding and is not transferred, are predicted to show pH-dependent enhancement with ΨiCαS in the NAIM assay (*30*). No such enhancement was observed at HDV C75. Instead, modest interference at a value slightly below what we have traditionally classified as significant persisted at all pHs between 5 and 8. The lack of ΨiCαS enhancement at C75 argues against a strictly structural role for the N3 proton of C75.

The data are consistent with a requirement for the proton to be transferred during the course of the cleavage reaction. ΨiCαS exists in two interchangeable tautomeric forms (Figure 5) (*30*, *36*−*38*). The primary tautomer is the N3−H form, which could serve as an uncharged protonated substitute for C. However, the high pK_a (pK_a = 9.4) of the N3 proton in this tautomeric form precludes efficient base ionization at neutral pH. This is consistent with the lack of enhancement and slight interference observed at C75. The relatively modest interference can be explained by the minor N1−H tautomer (Figure 5), which can substitute reasonably well for C because it has a hydrogen-bonding pattern and N3 pK_a (pK_a = 3.8) similar to the parental C (pK_a = 4.2) (*38*). The energetic cost of shifting into this tautomeric form could readily explain the modest interference effects. Alternatively, the slight ΨiCαS interference at C75 may result from the C−C bond in ΨiC that replaces the glycosidic linkage. This seems less likely because ΨiC is incorporated as efficiently as C by the RNA polymerase, and it does not cause interference at any other position within either the *Tetrahymena* group I intron or the HDV ribozyme. While glycosidic linkage is replaced with a C−C bond, the C−C bond distance is expected to be only 0.05 Å longer than the C−N bond (*48*). Thus, ΨiC appears to be a satisfactory substitute for C at the vast majority of positions in RNA. These data suggest that ΨiCαS interference in comparison to the other pK_a-perturbed C analogues could provide a simple means to qualitatively distinguish between structurally and catalytically important pK_a perturbations in RNA.

The first biochemical evidence for the use of proton transfer in the HDV cis-cleavage reaction came from imidazole-promoted rescue of the C75U mutant ribozyme (*18*, *29*). We have reported elsewhere that site-specific incorporation of 6-azauridine, a uridine analogue with a neutral pK_a, at nucleotide position 75 does not rescue ribozyme function (*49*). This suggested that the catalytic mechanism of the cis-cleavage of the HDV ribozyme is more complex than a simple placement of a base with histidine-like pK_a at the ribozyme active site.

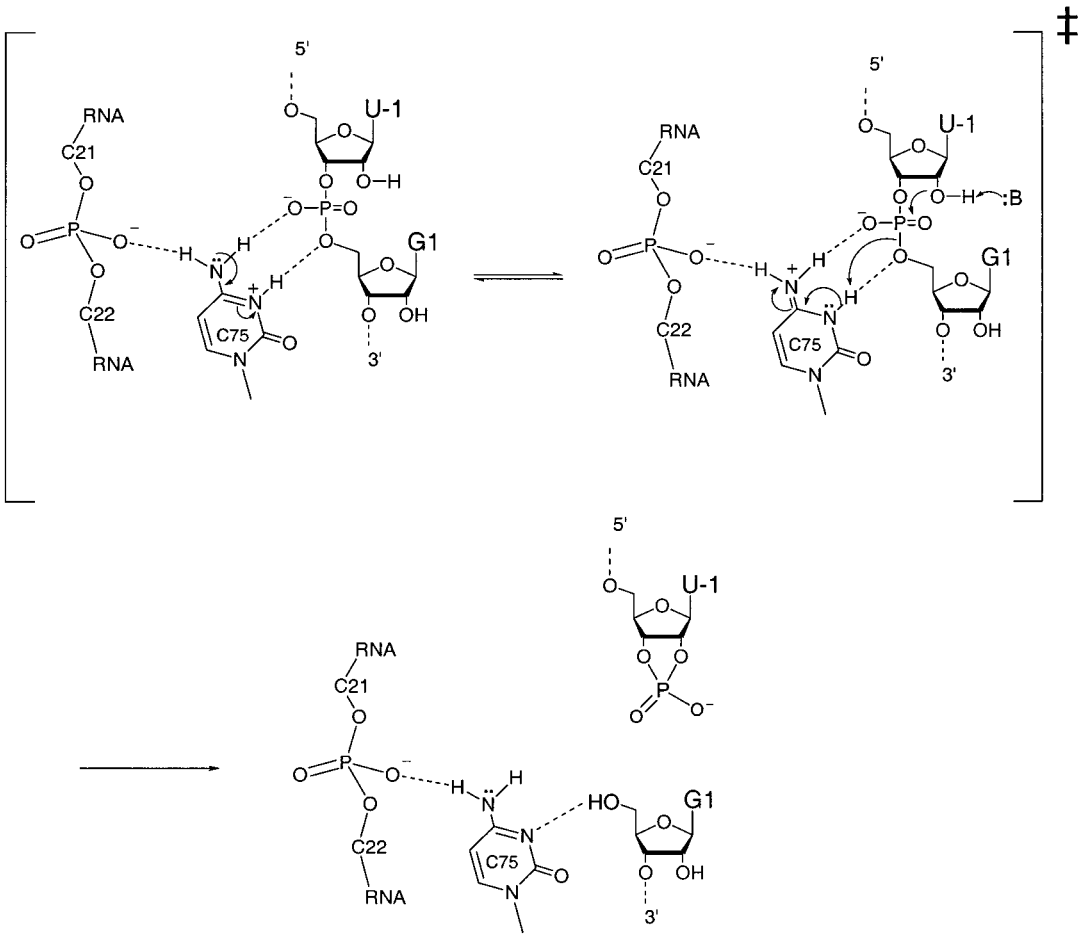

FIGURE 6: Proposed mechanism of pK_a perturbation and catalysis in the genomic HDV ribozyme. Hydrogen bonding between the *pro-*R_P phosphate oxygens of C22 and G1, the scissile phosphodiester bond, may contribute significantly to the imino tautomer and ground-state stabilization of the protonated C75. The cis-cleavage reaction may be initiated by specific base deprotonation of the 2′-OH group of U-1 followed by nucleophilic attack at the scissile phosphate. Charge redistribution in the transition state involving a proton transfer from the N3 of protonated C75 to the 5′-oxyanion leaving group drives the reaction equilibrium in favor of the cleavage products.

Within the crystal structure of the self-cleaved product of the genomic HDV ribozyme (*16*), the N3 of C75 is positioned in proximity to the 5′-oxygen of the leaving group. This geometric constraint combined with ΨiCαS interference suggests that the C75 may donate its N3 proton to relieve the developing charge on the leaving 5′-oxyanion group in the reaction transition state. Biochemical data from the cis-cleavage reaction of the genomic HDV ribozyme in high concentrations of Na^+ ions without divalent metal ions have been used to propose a similar model for general acid catalysis by C75 (*17*).

Model for the Mechanism of pK_a Perturbation. One useful consequence of this functional group analysis is an exploration of the critical interactions that may contribute to the pK_a perturbation at the C75 N3. A comparison of the present biochemical results with crystallographic data provides some clues as to how the HDV ribozyme uses proximity between an anionic phosphate oxygen and base functional groups to alter the electronic properties of the base. The self-cleaved ribozyme crystal structure revealed a hydrogen-bonding interaction between the *pro-*R_P oxygen of C22 and the trans face of the C75 N4 (*16*) (Figure 6). This hydrogen-bonding interaction is part of a network of interactions that organize the ribozyme active site (*16*). It may enhance the electron-donating potential of N4 into the heterocyclic ring, which would increase the basicity of C75 N3. Sulfur substitution at the *pro-*R_P position of C22 might be deleterious because it creates steric bulk that could potentially disrupt this interaction network. The phosphorothioate effect observed at C22 supports the formation of this hydrogen-bonding interaction within the ribozyme active site.

Although absent in the crystal structure, the only other phosphate oxygen that shows a metal ion-independent phosphorothioate effect is the *pro-*R_P oxygen of G1, the scissile phosphate (*16*, *47*). The *pro-*R_P oxygen of G1 may form a hydrogen-bonding interaction with the cis face of the C75 N4 group. The observed phosphorothioate effect at the G1 *pro-*R_P oxygen is at least consistent with this proposal. Additional evidence for the involvement of the *pro-*R_P oxygen of G1 in the hydrogen-bonding network comes from a recent NMR experiment. It was observed that the N3 pK_a of C75 in the self-cleaved ribozyme is not significantly altered compared to the free nucleoside (*50*). The inability of the self-cleaved ribozyme to induce N3 pK_a perturbation at C75 may be due to the lack of the G1 phosphate; i.e., the C75 pK_a is shifted in the precleaved state and/or the transition state, but it is not shifted in the cleaved state due to loss of the scissile phosphate.

The network of hydrogen-bonding interactions between the C22 *pro-*R_P oxygen, the C75 N4, and, potentially, the G1 *pro-*R_P oxygen could significantly enhance the stability of a protonated C75 (Figure 6). C analogues lacking the

connecting N4 group would not be able to perturb their N3 pK_as, and, thus, analogue incorporation should inhibit ribozyme function. Consistent with this possibility, incorporation of ZαS at C75 showed a pH-independent elimination of cis-cleavage activities. This result and the pH dependence of the interference by n^6CαS and f^5CαS, C analogues with N3 pK_as similar to ZαS, but having an intact N4 group, identify N4 as a vital chemical component through which the pK_a of the C75 N3 may be perturbed in the HDV ribozyme active site.

A model for the mechanism of pK_a perturbation in HDV ribozyme that is consistent with these results and other previously reported biochemical data is shown in Figure 6 (*17*, *18*). N3-protonated C75 is stabilized in the ground state by hydrogen-bonding interactions between its N4 group and *pro-*R_P oxygens of C22 and G1, anionic functional groups that define the ribozyme active site. Deprotonation of the 2′-OH group and ground-state destabilization through charge redistribution may provide a driving force for the cleavage reaction. The increase in proton-donating potential of C75 N3 as the RNA approaches the product state, revealed by the measured pK_a of the cleaved product (*50*), provides a further driving force that shifts the reaction equilibrium in favor of the cleaved products.

The proton-transfer mechanism of RNA catalysis may not be unique to the HDV ribozyme. Recent structural and biochemical studies suggested that the hairpin ribozyme may also utilize a base ionization event to catalyze a cis-cleavage reaction similar to that promoted by the HDV ribozyme (*51*, *52*). Furthermore, recent crystallographic data indicate that the ribosome is an RNA enzyme (*19*) and it might employ a pK_a-perturbed base, A2451, in the peptidyl transferase site to promote peptide bond formation (*19*, *21*).

Biochemical evidence presented here suggests how a microenvironment within a ribozyme active site may be used to activate functional groups for catalysis. The mechanism adopted by the HDV ribozyme is similar to that efficiently employed by protein enzymes to promote chemical reactions (*3*). Do RNAs use other protein enzyme-type mechanisms or adopt other mechanisms uniquely suited to their structures to effect charge-transfer catalysis? Detailed mechanistic studies on other ribozymes and ribonucleoprotein particles such as the ribosome, where charge-transfer catalytic mechanisms have been suggested, are essential to provide answers to these questions on the role of charge transfer in RNA catalysis.

ACKNOWLEDGMENT

We thank Lara Szewczak, Adrian R. Ferre-D'Amare, and Andrej Luptak for helpful discussion. We are grateful to Philip C. Bevilacqua for a gift of the genomic HDV plasmid.

SUPPORTING INFORMATION AVAILABLE

Figure 1a−c showing NAIM analysis of the HDV ribozyme in 1 M NaCl/1 mM EDTA at various pHs. This material is available free of charge via the Internet at http://pubs.acs.org.

REFERENCES

1. Silverman, R. B. (2000) *The Organic Chemistry of Enzyme-Catalyzed Reactions*, Academic Press, New York.
2. Blackburn, P., and Moore, S. (1982) in *The Enzymes* (Boyer, P. D., Ed.) pp 317−433, Academic Press, New York.
3. Westheimer, F. H. (1995) *Tetrahedron 51*, 3−20.
4. D'Alessio, G., and Riordan, J. F. (1997) in *RNases: Structures and Functions*, Academic Press, New York.
5. Narlikar, G. J., and Herschlag, D. (1997) *Annu. Rev. Biochem. 66*, 19−59.
6. Kruger, K., Grabowski, P. J., Zaug, A. J., Sands, J., Gottschling, D. E., and Cech, T. R. (1982) *Cell 31*, 147−157.
7. McKay, D. B., and Wedekind, J. E. (1999) in *The RNA World* (Gesteland, R. F., Cech, T. R., and Atkins, J. F., Eds.) pp 265−286, Cold Spring Harbor Laboratory Press, Cold Spring Harbor, NY.
8. Cech, T. R., and Golden, B. L. (1999) in *The RNA World* (Gesteland, R. F., Cech, T. R., and Atkins, J. F., Eds.) pp 321−349, Cold Spring Harbor Laboratory Press, Cold Spring Harbor, NY.
9. Saenger, W. (1984) *Principles of Nucleic Acid Structure*, Springer-Verlag, New York.
10. Wang, C., Gao, H., Gaffney, B. L., and Jones, R. A. (1991) *J. Am. Chem. Soc. 113*, 5486−5488.
11. Leroy, J. L., Gehring, K., Kettani, A., and Gueron, M. (1993) *Biochemistry 32*, 6019−6031.
12. Legault, P., and Pardi, A. (1994) *J. Am. Chem. Soc. 116*, 8390−8391.
13. Legault, P., and Pardi, A. (1997) *J. Am. Chem. Soc. 119*, 6621−6628.
14. Ravindranathan, S., Butcher, S. E., and Feigon, J. (2000) *Biochemistry 39*, 16026−16032.
15. Singleton, S. F., and Dervan, P. B. (1992) *Biochemistry 31*, 10995−11003.
16. Ferre-D'Amare, A. R., Zhou, K. H., and Doudna, J. A. (1998) *Nature 395*, 567−574.
17. Nakano, S., Chadalavada, D. M., and Bevilacqua, P. C. (2000) *Science 287*, 1493−1497.
18. Perrotta, A. T., Shih, I. H., and Been, M. D. (1999) *Science 286*, 123−126.
19. Nissen, P., Hansen, J., Ban, N., Moore, P. B., and Steitz, T. A. (2000) *Science 289*, 920−930.
20. Ban, N., Nissen, P., Hansen, J., Moore, P. B., and Steitz, T. A. (2000) *Science 289*, 905−920.
21. Muth, G. W., Ortoleva-Donnelly, L., and Strobel, S. A. (2000) *Science 289*, 947−950.
22. Nesbitt, S., Hegg, L. A., and Fedor, M. J. (1997) *Chem. Biol. 4*, 619−630.
23. Earnshaw, D. J., and Gait, M. J. (1998) *Nucleic Acids Res. 26*, 5551−5561.
24. Murray, J. B., Seyhan, A. A., Walter, N. G., Burke, J. M., and Scott, W. G. (1998) *Chem. Biol. 5*, 587−595.
25. Lai, M. M. (1995) *Annu. Rev. Biochem. 64*, 259−286.
26. MacNaughton, T. B., Wang, Y.-J., and Lai, M. M. C. (1993) *J. Virol. 67*, 2228−2234.
27. Been, M. D., and Wickham, G. S. (1997) *Eur. J. Biochem. 247*, 741−753.
28. Wadkins, T. S., Perrotta, A. T., Ferre-D'Amare, A. R., Doudna, J. A., and Been, M. D. (1999) *RNA 5*, 720−727.
29. Shih, I., and Been, M. D. (2001) *Proc. Natl. Acad. Sci. U.S.A. 98*, 1489−1494.
30. Oyelere, A. K., and Strobel, S. A. (2000) *J. Am. Chem. Soc. 122*, 10259−10267.
31. Jonas, J., and Gut, J. (1962) *Collect. Czech. Chem. Commun. 27*, 716.
32. Wempen, I., Fox, J. J., Kaplan, L., and Duschinsky, R. (1961) *J. Am. Chem. Soc. 83*, 4755.
33. Scheit, K. H. (1980) *Nucleotide Analogues: Synthesis and Biological Function*, John Wiley & Sons, New York.
34. Brown, D. J. (1962) in *The Chemistry of Heterocyclic Compounds* (Weissberger, A., Ed.) pp 464−500, John Wiley & Sons, New York.
35. Gildea, B., and McLaughlin, L. W. (1989) *Nucleic Acids Res. 17*, 2261−2281.
36. Ono, A., Tso, P. O. P., and Kan, L. S. (1991) *J. Am. Chem. Soc. 113*, 4032−4033.

37. Ono, A., Tso, P. O. P., and Kan, L. S. (1992) *J. Org. Chem. 57*, 3225−3230.
38. Kan, L. S., Lin, W. C., Yadav, R. D., Shih, J. H., and Chao, I. (1999) *Nucleosides Nucleotides 18*, 1091−1093.
39. Szewczak, A. A., Ortoleva-Donnelly, L., Zivarts, M. V., Oyelere, A. K., Kazantsev, A. V., and Strobel, S. A. (1999) *Proc. Natl. Acad. Sci. U.S.A. 96*, 11183−11188.
40. Wadkins, T. S., Shih, I. H., Perrotta, A. T., and Been, M. D. (2001) *J. Mol. Biol. 305*, 1045−1055.
41. Arabshahi, A., and Frey, P. A. (1994) *Biochem. Biophys. Res. Commun. 204*, 150−155.
42. Huang, Z., and Szostak, J. W. (1996) *Nucleic Acids Res. 24*, 4360−4361.
43. Hausner, T. P., Giglio, L. M., and Weiner, A. M. (1990) *Genes Dev. 4*, 2146−2156.
44. Strobel, S. A., and Shetty, K. (1997) *Proc. Natl. Acad. Sci. U.S.A. 94*, 2903−2908.
45. Strobel, S. A. (1999) *Cur. Opin. Struct. Biol. 9*, 346−352.
46. Ryder, S. P., Ortoleva-Donnelly, L., Kosek, A. B., and Strobel, S. A. (2000) *Methods Enzymol. 317*, 92−109.
47. Jeoung, Y. H., Kumar, P. K. R., Suh, Y. A., Taira, K., and Nishikawa, S. (1994) *Nucleic Acids Res. 22*, 3722−3727.
48. March, J. (1992) *Advanced Organic Chemistry*, John Wiley & Sons, New York.
49. Oyelere, A. K., and Strobel, S. A. (2001) *Nucleosides Nucleotides 20*, 1851−1858.
50. Luptak, A., Ferre-D'Amare, A. R., Zhou, K., Zilm, K. W., and Doudna, J. A. (2001) *J. Am. Chem. Soc. 123*, 8447−8452.
51. Rupert, P. B., and Ferre-D'Amare, A. R. (2001) *Nature 410*, 780−786.
52. Ryder, S. P., Oyelere, A. K., Padilla, J. L., Klostermeier, D., Millar, D. P., and Strobel, S. A. (2001) *RNA 7*, 1454−1463.

BI011816V